The ISME Journal (2020) 14:2732–2747
https://doi.org/10.1038/s41396-020-0725-0

ARTICLE

Anoxygenic photosynthesis and iron–sulfur metabolic potential of *Chlorobia* populations from seasonally anoxic Boreal Shield lakes

J. M. Tsuji[1] · N. Tran[1] · S. L. Schiff[1] · J. J. Venkiteswaran[1,2] · L. A. Molot[3] · M. Tank[4,5] · S. Hanada[5] · J. D. Neufeld[1]

Received: 28 May 2019 / Revised: 2 July 2020 / Accepted: 20 July 2020 / Published online: 3 August 2020
© The Author(s), under exclusive licence to International Society for Microbial Ecology 2020

Abstract

Aquatic environments with high levels of dissolved ferrous iron and low levels of sulfate serve as an important systems for exploring biogeochemical processes relevant to the early Earth. Boreal Shield lakes, which number in the tens of millions globally, commonly develop seasonally anoxic waters that become iron rich and sulfate poor, yet the iron–sulfur microbiology of these systems has been poorly examined. Here we use genome-resolved metagenomics and enrichment cultivation to explore the metabolic diversity and ecology of anoxygenic photosynthesis and iron/sulfur cycling in the anoxic water columns of three Boreal Shield lakes. We recovered four high-completeness and low-contamination draft genome bins assigned to the class *Chlorobia* (formerly phylum *Chlorobi*) from environmental metagenome data and enriched two novel sulfide-oxidizing species, also from the *Chlorobia*. The sequenced genomes of both enriched species, including the novel "*Candidatus* Chlorobium canadense", encoded the *cyc2* gene that is associated with photoferrotrophy among cultured *Chlorobia* members, along with genes for phototrophic sulfide oxidation. One environmental genome bin also encoded *cyc2*. Despite the presence of *cyc2* in the corresponding draft genome, we were unable to induce photoferrotrophy in "*Ca*. Chlorobium canadense". Genomic potential for phototrophic sulfide oxidation was more commonly detected than *cyc2* among environmental genome bins of *Chlorobia*, and metagenome and cultivation data suggested the potential for cryptic sulfur cycling to fuel sulfide-based growth. Overall, our results provide an important basis for further probing the functional role of *cyc2* and indicate that anoxygenic photoautotrophs in Boreal Shield lakes could have underexplored photophysiology pertinent to understanding Earth's early microbial communities.

Introduction

Precambrian Shield regions in northern areas globally contain millions of small humic lakes [1–3]. Many of these Boreal Shield lakes develop a seasonally anoxic water column that becomes ferruginous, dominated by dissolved ferrous iron compared to sulfate and sulfide [4, 5]. However, little is known about the iron and sulfur microbiology of seasonally anoxic and ferruginous Boreal Shield lake systems. Several studies have examined the role of phototrophic members of the class *Chlorobia* (formerly phylum *Chlorobi* [6]; also called "green sulfur bacteria") in boreal lake waters (e.g., [7]), because these organisms are commonly found at high relative abundances in the illuminated and anoxic water columns of boreal lakes. *Chlorobia* members are typically assumed to use a reduced sulfur compound, such as sulfide or thiosulfate, as their photosynthetic electron donor [8, 9]. However, recent cultivation-based discoveries have expanded the known metabolic diversity of anoxygenic photosynthesis to include the

Supplementary information The online version of this article (https://doi.org/10.1038/s41396-020-0725-0) contains supplementary material, which is available to authorized users.

✉ J. D. Neufeld
jneufeld@uwaterloo.ca

[1] University of Waterloo, 200 University Avenue West, Waterloo, ON N2L 3G1, Canada

[2] Wilfrid Laurier University, 75 University Avenue West, Waterloo, ON N2L 3C5, Canada

[3] York University, 4700 Keele Street, Toronto, ON M3J 1P3, Canada

[4] Leibniz Institute DSMZ-German Collection of Microorganisms and Cell Cultures GmbH, Inhoffenstrasse 7B, 38124 Braunschweig, Germany

[5] Tokyo Metropolitan University, 1-1 Minami-osawa, Hachioji, Tokyo 192-0397, Japan

photosynthetic oxidation of compounds such as ferrous iron, arsenate, and nitrite, and these alternative metabolic modes of photosynthesis challenge classical interpretations of how anoxic ecosystems function [10–13].

Among the *Chlorobia* class, diverse ferrous iron-oxidizing phototrophs, also called photoferrotrophs, have been cultivated recently. Previously, the only known photoferrotroph in this group was *Chlorobium ferrooxidans* strain KoFox, which was enriched from freshwater lake sediments [14]. Recently, *Chlorobium phaeoferrooxidans* strain KB01, a bacteriochlorophyll *e*-containing member of the class *Chlorobia*, was isolated from the anoxic water column of the meromictic and ferruginous Kabuno Bay [15]. In addition, *Chlorobium* sp. strain N1 was enriched from marine sediments [16]. Both *Chl. ferrooxidans* and *Chl. phaeoferrooxidans* oxidize ferrous iron as their sole photosynthetic electron donor, assimilating sulfur as sulfate [14, 15]. *Chl*. sp. N1 is capable of oxidizing either ferrous iron or sulfide as the photosynthetic electron donor and can also utilize organic compounds [16]. A fourth recently isolated photoferrotroph, *Chlorobium* sp. BLA1, was shown to also be capable of oxidizing sulfide, although genome data are not yet available for this strain [17]. Phylogenetically, *Chl. ferrooxidans* and *Chl. phaeoferrooxidans* are sister groups to one another, whereas *Chl*. sp. N1 is closely related to *Chl. luteolum*, a sulfide-oxidizing species of *Chlorobia* hypothesized to be able to switch to photoferrotrophic growth [15, 16, 18]. These cultivation-based discoveries have highlighted the potential metabolic diversity and flexibility of *Chlorobia* members. Discovery of additional photoferrotrophs has also stimulated discussion around the potential involvement of photoferrotrophs in early Earth microbial communities, such as the ferruginous water columns of Archaean Eon oceans (ca. 3.8–2.5 Ga) [15, 19, 20].

Despite growing evidence for the metabolic diversity of anoxygenic photosynthesis, the ecology of photoferrotrophy and other alternative photosynthetic modes remains poorly understood. One of the key challenges in assessing the modern importance of photoferrotrophy has been a limited understanding of the biochemistry and genetics of iron oxidation. Recent work has begun to unravel the molecular basis for iron oxidation in photoferrotrophs and other neutrophilic iron-oxidizing bacteria (reviewed in [21, 22]). Genes encoding for porin-cytochrome *c* protein complexes (PCC), such as *pioAB* and *mtoAB*, have been identified as potentially useful markers for iron oxidation in some species [22–24]. In addition, genes encoding for outer-membrane monoheme c-type cytochromes, such as *cyc2*, have received recent interest for their role in extracellular electron transfer, with proteomic and RNA-seq studies indicating a role for such genes in microaerophilic iron oxidation [25–27]. Among the *Chlorobia*, genome sequences available for *Chl. ferrooxidans*, *Chl. phaeoferrooxidans*, *Chl*. sp. N1, and *Chl. luteolum* show that their genomes encode *cyc2* homologs, unlike all other sulfide-oxidizing *Chlorobia* members [18, 28–30], providing preliminary evidence that *cyc2* might serve as a genomic marker for photoferrotrophy within the class *Chlorobia*. Confirming the validity of candidate iron oxidation gene markers such as *cyc2* for photoferrotrophic metabolism would greatly expand the potential to survey for photoferrotrophy and other forms of extracellular electron transfer in nature.

Here, we combine genome-resolved metagenomics and enrichment cultivation to probe the metabolic diversity of anoxygenic phototrophs in seasonally anoxic and ferruginous Boreal Shield lakes, particularly examining the potential for photoferrotrophy. Following up initial 16S ribosomal RNA (16S rRNA) gene sequencing and iron isotope data that led us to hypothesize photoferrotrophy as an important photosynthetic process in the water columns of two Boreal Shield lakes, we recover high-completeness, low-contamination draft genomes of key populations of *Chlorobia*, the dominant anoxygenic phototrophs, from the same two lakes. We also report the enrichment of two novel species of *Chlorobia* from these lakes and from a third Boreal Shield lake, and we analyze the genetic and functional potential of these species for phototrophic sulfide and iron oxidation. Lastly, we explore the usage of *cyc2* as a functional gene marker for photoferrotrophy compared to other phototrophic modes. Through this first usage of genome-resolved metagenomics to explore the metabolic diversity of *Chlorobia* in a ferruginous water column, we aim to extend sparse knowledge of iron–sulfur microbiology in ferruginous lake systems, with implications for understanding both Archaean microbial communities and modern ferruginous environments.

Materials and methods

Lake sampling, metagenome sequencing, assembly, and binning

An initial round of lake sampling was performed previously from 2011 to 2014 at the International Institute for Sustainable Development Experimental Lakes Area (IISD-ELA; near Kenora, Canada), which is located at 49°40′N, 93°45′W [4]. We studied Lake 227, an experimentally eutrophied lake, and Lake 442, a nearby and pristine reference lake [31, 32]. The IISD-ELA sampling site, lake geochemistry, and sample collection methods were described in detail previously [4]. Based on preliminary 16S rRNA gene data, we selected six water column genomic DNA samples collected from Lakes 227 and 442 for

re-sequencing via shotgun metagenomics. All six samples were collected at or beneath the oxic–anoxic zone boundary, at depths where low light penetration occurs, and where we had previously observed high relative abundances of anoxygenic phototrophs, dominated by populations of *Chlorobia*. Samples from Lake 227 were selected at 6 and 8 m in 2013 and 2014, and samples from Lake 442 were selected at 16.5 m in 2011 and 13 m in 2014. The sequencing library was prepared using the NEBNext Ultra II DNA Library Prep Kit for Illumina (New England Biolabs; Ipswich, Massachusetts, USA) and was sequenced on a single lane of a HiSeq 2500 (Illumina; San Diego, California, USA) in Rapid Run Mode with 2×200 base paired-end reads, generating 26.3–39.5 million reads per sample. Library preparation and sequencing was performed by the McMaster Genome Facility (Hamilton, Ontario, Canada).

Raw metagenome reads were quality-trimmed, assembled, binned, and annotated using the ATLAS pipeline, version 1.0.22 [33, 34]. The configuration file with all settings for the pipeline is available in Supplementary File 1. To improve genome bin completeness and reduce bin redundancy, QC processed reads from related samples (i.e., L227 2013 6 and 8 m, L227 2014 6 and 8 m, and L442 samples) were co-assembled and re-binned using differential abundance information via a simple wrapper around ATLAS, as described in the Supplementary Methods.

Identification of *cyc2* genes and *Chlorobia* genome bins

Assembled contigs were assessed for the presence of *cyc2* gene homologs by building a custom profile hidden Markov model (HMM). The predicted primary sequences of *cyc2* were recovered from the four available genomes of *Chlorobia* known to possess the gene, *Chl. ferrooxidans*, *Chl. phaeoferrooxidans*, *Chl*. sp. N1, and *Chl. luteolum*, as well as from the genomes of reference microaerophilic iron-oxidizing bacteria as described elsewhere [21]. A cytochrome 572 gene from *Leptospirillum* sp. (EDZ39515.1) was omitted from the reference dataset, due to its high divergence from other sequences, to build a more robust alignment for the *cyc2* clade relevant to the *Chlorobia* [35]. Collected sequences were aligned using Clustal Omega, version 1.2.3 [36], and the alignment was used to build a profile HMM using the *hmmbuild* function of HMMER3, version 3.2.1 [37]. Recovered *cyc2* genes over the course of the study were added to the alignment and HMM. The final HMM is provided in Supplementary File 2 and sequence alignments are available in the code repository associated with this work.

Recovered *cyc2* genes were compared to *cyc2* reference sequences by building a maximum-likelihood phylogeny. The alignment was masked using Gblocks, version 0.91b [38], as described in the Supplementary Methods. The maximum-likelihood phylogeny was then prepared from the masked sequence alignment via IQ-TREE, version 1.6.10 [39], using the $LG + F + I + G4$ sequence evolution model as determined by the ModelFinder module of IQ-TREE [40]. To build the consensus tree, 1000 bootstrap replicates were performed, each requiring ~100–110 tree search iterations for phylogeny optimization.

Genome bins were dereplicated using dRep version 2.0.5 [41] with default settings. All genome bins from individual assembles and co-assemblies were pooled for dereplication to help ensure that the highest quality bins, whether from individual assemblies or co-assemblies, would be retained for downstream analyses. Genome bins of *Chlorobia* with >90% completeness and <10% contamination based on CheckM statistics [42] were selected for further study. These genome bins were imported into Anvi'o version 4 [43] and were manually examined for contigs improperly binned based on read mapping, tetranucleotide frequencies, and contig taxonomic classification. Import of ATLAS data into Anvi'o was performed using the *atlas-to-anvi.sh* script, version 1.0.22-co-assembly-r4, available in the *atlas-extensions* GitHub repository at https://github.com/jmtsuji/atlas-extensions. Contigs in curated genome bins of *Chlorobia* were then ordered via the Mauve Contig Mover development snapshot 2015-02-13 for Linux [44] using the *Chl. luteolum* genome to guide ordering. To assess bin quality, tRNA genes were predicted using Prokka v1.13.3 [45].

Enrichment cultivation, sequencing, and assembly

Lake 227 and Lake 442 were sampled again in June 2016 and July 2017, along with the nearby Lake 304 in July 2017. Basic sampling information for each lake is summarized in Supplementary Table 1. Lake 304 has been described previously and also has seasonally anoxic bottom waters [46, 47]. The lake was experimentally fertilized with phosphate in 1971–72 and 1975–76, with ammonium in 1971–74, and with nitrate in 1973–74, but the lake has not been manipulated since then and rapidly returned to its non-eutrophied state once additions ceased, having a water residence time of ~2.7 years [48–50]. Lake 304 was added to our sampling efforts for enrichment culturing to explore the broader distribution of photoferrotrophy among IISD-ELA lakes, because preliminary 16S rRNA gene sequencing data (not shown) indicated high relative abundances of *Chlorobia* populations in this lake. Anoxic water was collected from Lakes 227 and 304 at a depth of 6 m and Lake 442 at 15 m, where trace levels of light are generally detectable (i.e., in the range of 0.01–1 µmol photons m^{-2} s^{-1} between 400 and 700 nm wavelengths, as commonly measured when field sampling). Lake water was pumped to the surface using a

gear pump and directly injected into N_2-filled 160 mL glass serum bottles that were sealed with blue butyl rubber stoppers (Bellco Glass; Vineland, New Jersey, USA), using a secondary needle to vent N_2 gas until the bottles were full. Water was kept cold (~4 °C) and dark after collection and during shipping.

Enrichment cultures were grown using sulfide-containing Pfennig's medium, prepared as described by Imhoff [8, 9], or ferrous iron-containing freshwater medium, prepared as described by Hegler et al. [51]. The ferrous iron-containing medium contained 8 mM ferrous chloride ($FeCl_2$), without filtration of precipitates, and used trace element solution SLA [8]. Initial enrichments contained 10–20% lake water at a total volume of 50 mL and were inoculated into 120–160 mL glass serum bottles sealed with blue butyl rubber stoppers (Bellco Glass) or black rubber stoppers (Geo-Microbial Technology Company; Ochelata, Oklahoma, USA). The remaining headspace was flushed with a 90:10 N_2:CO_2 gas mix at left at a pressure of 150 kPa. Several bottles additionally had anoxic DCMU (i.e., Diuron or 3-(3,4-dichlorophenyl)-1,1-dimethylurea; Sigma-Aldrich; St. Louis, Missouri, USA) added to a concentration of 50 µM to block activity of oxygenic phototrophs [52, 53]. Bottles were incubated at 22 °C and ~50 cm away from far red PARSource PowerPAR LED Bulbs (LED Grow Lights Depot; Portland, Oregon, USA) as the light source.

Two enrichment cultures survived repeated subculture or dilution-to-extinction and contained green sulfur bacteria based on pigment and marker gene sequence analyses. Biomass from these cultures was collected by centrifugation, and genomic DNA was extracted using the DNeasy UltraClean Microbial Kit (Qiagen; Venlo, The Netherlands). Genomic DNA was prepared into metagenome sequencing libraries using the Nextera DNA Flex Library Prep Kit (Illumina), and the library was sequenced on a fraction of a HiSeq 2500 (Illumina) lane in High Output Run Mode with 2 × 125 base paired-end reads. Library preparation and sequencing was performed by The Center for Applied Genomics (TCAG; The Hospital for Sick Children, Toronto, Canada), generating ~6 million total reads per sample. Metagenomes were assembled using ATLAS version 1.0.22 without co-assembly. Genome bins of *Chlorobia* were manually refined as described above, using Anvi'o version 5 [43] via *atlas-to-anvi.sh* commit 99b85ac; contigs of curated bins were subsequently ordered, and tRNA genes counted, as described above.

Comparative genomics of *Chlorobia* genomes

Refined genome bins of *Chlorobia*, which belonged to the *Chlorobium* genus, were compared to genomes of reference strains from the *Chlorobiaceae* family. Genomes of all available type strains (as of 2017) and photoferrotrophs from the family were downloaded from the NCBI (Supplementary File 3). Average nucleotide identity (ANI) between genomes was calculated using FastANI version 1.1 [54]. The phylogenetic relationship between genomes was determined by constructing a concatenated ribosomal protein alignment based on the rp1 set of 16 ribosomal protein genes using GToTree version 1.1.10 [55, 56]. IQ-TREE version 1.6.9 [39] was used to construct the maximum-likelihood phylogeny from the alignment. The LG + F + R4 model of sequence evolution was identified as optimal by the IQ-TREE ModelFinder module [33], and phylogeny construction used 1000 bootstrap replicates, each requiring ~100–110 tree search iterations for optimization.

The presence or absence of genes implicated in iron or sulfur cycling metabolism in the collection of *Chlorobiaceae* genomes was assessed using bidirectional BLASTP [57]. Genes were selected from the genomes of *Chl. ferrooxidans* and *Chl. clathratiforme* based on the genome comparison of Frigaard and Bryant [18]. Predicted primary sequences of these genes were used to identify putative homologs across other genomes of *Chlorobia* using the BackBLAST pipeline, version 2.0.0-alpha2 (https://doi.org/10.5281/zenodo.3465955) [58]. The *e* value cutoff for BLASTP hits was set at 10^{-40}, based on empirical testing of gene clusters known to be present or absent in reference genomes of *Chlorobia*, and the identity cutoff was set to 20%. Selected genes (e.g., *qmoA*, *dsrJ*) were omitted due to poor homology between reference genomes. Genes associated with photosynthesis and carbon fixation were similarly assessed using BackBLAST, except that most reference genes were selected from the genome of *Chl. tepidum* according to Bryant et al. [59] and Tourova et al. [60].

Metagenome taxonomic and functional profiling

Environmental relative abundances of microbial populations were estimated by read mapping to dereplicated genome bins (further details in Supplementary Methods). Taxonomy and functional gene information were then overlaid onto relative abundance data. Genome bin taxonomy was determined based on the Genome Taxonomy Database (GTDB) using GTDB-Tk, version 0.2.2, relying on GTDB release 86, version 3 (April 2019) [6, 61]. As such, GTDB taxonomy names are used throughout this paper. Genomes were tested for the presence of the *cyc2* and *dsrA* functional genes using the HMM developed in this study and an HMM available on FunGene [62], respectively. Gene amino acid translations were predicted for all genome bins using prodigal version 2.6.3 [63], via the GTDB-Tk, and amino acid translations were searched via HMMs using the MetAnnotate pipeline, version 0.9.2 [64]. An *e* value cutoff of 10^{-40} was used to filter low-quality

gene hits. In case of bias due to unassembled or incorrectly binned genes, genome bin-based environmental abundance metrics were cross compared to abundance metrics generated by directly scanning unassembled metagenome reads, as described in the Supplementary Methods. Genome bins were further assessed for their broader iron- and sulfur-cycling genomic potential using additional gene markers and FeGenie [65] commit 30174bb, as described in the Supplementary Methods.

Assessment of ferrous iron oxidation potential of *Chlorobia* enrichments

After initial sequencing, cultures containing *Chlorobia* spp. continued to be purified in the laboratory. A single culture, which was enriched on sulfide-containing medium, survived continued cultivation and was provisionally named "*Candidatus* Chlorobium canadense strain L304-6D" (ca.na. den'se N.L. neut. adj. *canadense* from or belonging to Canada). "*Ca*. Chl. canadense" was purified through multiple rounds of incubation in deep agar dilution series and picking of isolated green colonies [66]. For deep agar shakes, Pfennig's medium or modified *Chloracidobacterium thermophilum* Midnight medium [67] containing 1–3 mM buffered sulfide feeding solution were used [8]. Eventually, in preparation for growth in ferrous iron-containing medium, cultures of "*Ca*. Chl. canadense" were transferred to growth in liquid freshwater medium as described by Hegler et al. [51] (here termed, "Hegler freshwater medium") but containing 0.5–1 mM buffered sulfide feeding solution, 10–20 µM $FeCl_2$, and 0.5 mg/L resazurin to monitor the medium's redox status.

To test their ability to oxidize ferrous iron phototrophically, "*Ca*. Chl. canadense" cells were inoculated into Hegler freshwater medium containing low levels of ferrous iron and lacking sulfide. The base Hegler freshwater medium (before addition of ferrous iron or sulfide) was aliquoted into 120 mL glass serum bottles under flow of sterile 90:10 N_2:CO_2 gas, with 50 mL of medium per bottle. Bottles were sealed with black rubber stoppers (Geo-Microbial Technology Company) and were bubbled for at least 9 min with additional 90:10 N_2:CO_2 gas to purge trace oxygen. The headspace of each bottle was left at 150 kPa pressure. A sterile solution of $FeCl_2$ was added to each bottle to reach a ferrous iron content of 100 µM, and to some bottles, a sterile and anoxic solution of the chelator ethylenediaminetetraacetic acid (EDTA) was added to a concentration of 120 µM as done by Peng et al. [68] to explore whether this chelator could enhance photoferrotrophic iron oxidation. Bottles were incubated at room temperature in the dark overnight to allow for complexation of ferrous iron and EDTA. All media was confirmed to have a pH of 6.5–7.

"*Ca*. Chl. canadense" was grown in 100 mL Hegler freshwater medium using a total of ~2 mM sulfide, fed incrementally in 0.4 mM doses, until sulfide was completely oxidized and the resazurin in the bottle went slightly pink. At the same time, a culture of *Chl. ferrooxidans* KoFox was grown in the same freshwater medium containing ~8 mM $FeCl_2$ until ferrous iron was completely oxidized. The entire 100 mL "*Ca*. Chl. canadense" culture was pelleted by centrifugation at 7000 × *g* for 13 min, and the pellet was washed twice with unamended Hegler freshwater medium. The ~200 mg of wet biomass recovered was suspended in 1 mL of unamended freshwater medium, and 0.1 mL was inoculated into each relevant incubation bottle. Similarly, 100 mL of the *Chl. ferrooxidans* reference culture was pelleted by centrifugation at 7000 × *g* for 5 min, washed twice, and suspended in 1 mL of unamended freshwater media, and 0.1 mL was added to relevant bottles. Only the surfaces of *Chl. ferrooxidans* cell pellets, which contained mostly green cells and not brown ferric iron precipitate, were suspended with each wash, allowing for ~3 mg of nearly iron-free wet biomass to be recovered. Once cultures were inoculated, they were transferred to a 22 °C incubator without shaking where they received 30 µmol photons m^{-2} s^{-1} white light from a mix of fluorescent (F48T12/CW/VHO; Osram Sylvania; Wilmington, Massachusetts, USA) and incandescent (60 W) bulbs.

Cultures were sampled regularly over a 21-day incubation period to monitor iron concentrations and iron oxidation states. At each sampling time point, an aliquot of culture was removed from each bottle using a sterile 90:10 N_2:CO_2-flushed syringe and 25 G needle, and 330 µL of this culture aliquot was acidified immediately with 30 µL of 6 N hydrochloric acid (HCl). Acidified samples were stored for no more than 2 days at 4 °C (with the exception of samples collected on day 14; see Supplementary Methods) before being assessed for iron species concentrations via the ferrozine assay [69], with 5% ascorbic acid being used as the reducing agent to determine total iron species [70].

Results

Recovery of *Chlorobium* genome bins

Binning of assembled contigs from the lake and enrichment culture metagenomes, followed by dereplication of highly similar bins and manual curation, allowed for the recovery of six highly complete, low-contamination genome bins that classified within the genus *Chlorobium* (Table 1). Three of the genome bins recovered from lake metagenomes had best representatives selected by dRep from the Lake 227 (2013 sample) co-assembly, and one had its best representative from the Lake 442 (2011/2014 sample)

Table 1 Quality statistics for genome bins of *Chlorobia* recovered in this study.

Bin ID	Contigs	Length (Mb)	N50 (kb)	L50	GC content (%)	Genes	tRNA genes	Completeness (%)	Contamination (%)
L227 2013 Bin 55	208	2.38	16.7	42	48.5	2397	39	97.4	0.1
L227 2013 Bin 56	140	2.09	27.6	21	43.9	2009	38	96.7	0.6
L227 2013 Bin 22	57	2.55	79.5	12	45.9	2471	37	98.5	2.8
L442 Bin 64	128	1.90	28.6	22	48.3	1871	35	90.1	0.0
L227 enr. S-6D Bin 1	13	2.50	306.7	3	46.8	2385	44	99.5	1.0
Ca. Chl. canadense L304-6D	15	2.61	271.5	3	48.7	2504	45	99.4	0.0

Completeness and contamination were calculated using CheckM (see "Methods"). Note that no ribosomal RNA genes were recovered for the bins. A summary of bin statistics for lower-quality genome bins is included in Supplementary File 4.

co-assembly. In addition, a single *Chlorobium* genome bin was recovered from each enrichment culture. Recovered bins had at least 90.1% completeness and a maximum of 2.8% contamination based on analysis by CheckM [42]. Recovered genome bins were between 1.9 and 2.6 Mb in size, within the approximate length range of reference genomes associated with the family *Chlorobiaceae* (2.0–3.3 Mb; average 2.7 Mb), and were represented by 13–208 contigs. Other lower-quality genome bins classified as belonging to the *Chlorobia* were also recovered (Supplementary File 4), but these were not considered for gene pathway analysis in order to minimize the risk of including false positives. In particular, L442 Bin 74 was excluded from the set of curated bins due to its high contig count (282) and elevated predicted contamination (4.1%) and strain heterogeneity (25%).

The constructed HMM for the *cyc2* gene enabled the recovery of five potential *cyc2* homologs associated with *Chlorobia* from assembled contigs (Fig. 1). Three of these *cyc2* homologs were found in the set of six manually curated genome bins described above, and another homolog was detected in one of the lower-quality genome bins of *Chlorobia* (L227 2014 Bin 92). The final homolog was detected on a short contig in the same lower-quality genome bin and was removed from subsequent analyses due to its lack of gene neighbors. Detected *cyc2* homologs were full-length genes, and their predicted primary sequences were detected in the HMM search with a maximum *e* value of ~10^{-140}. All recovered *cyc2* homologs contained the heme-binding CXXCH motif near the N-terminus of their predicted primary sequence, and all homologs were predicted by I-TASSER [71] to contain a porin-like beta barrel structure for membrane binding (Fig. 1a; one example shown) [13]. Aside from the closely related genomes of *Chl. ferrooxidans* and *Chl. phaeoferrooxidans* (Supplementary Fig. 1), all other genomes showed substantial genome rearrangement around the *cyc2* homolog (Fig. 1b). However, detected *cyc2* homologs were always adjacent to a *c5* family cytochrome (Fig. 1b). These *c5* family cytochromes had low sequence identity to one another (i.e., as low as 30%) yet also contained a conserved CXXCH motif (Supplementary Fig. 2). All recovered *cyc2* homologs grouped monophyletically with *cyc2* predicted primary sequences belonging to reference genomes of *Chlorobia* compared to the *cyc2* of other reference strains (Fig. 1c). Overall, the combination of HMM search specificity, genomic context, predicted gene motifs, and phylogenetic placement is strong evidence that the identified cytochrome genes are *cyc2* homologs.

Enrichment cultivation of *Chlorobia*

Enrichment cultivation was attempted with anoxic lake water using both sulfide- and ferrous iron-containing anoxic media. For Lake 442, one enrichment in a ferrous iron-containing medium grew with evidence of light-driven iron oxidation, but 16S rRNA gene sequencing showed that the culture was dominated by a member of the genus *Rhodopseudomonas*, which did not represent a detectable genus in environmental sequencing data. Given the known metabolic versatility of *Rhodopseudomonas* spp. and the negligible contribution of members of this genus to the studied lake microbial communities, this culture was not pursued further. No members of the *Chlorobia* were detected in any enrichment culture from Lake 442.

For Lakes 227 and 304, growth was observed for both media tested. Enrichments grown in sulfide-containing medium developed green color after ~12–15 weeks of incubation and contained populations of *Chlorobia* based on Sanger sequencing of both the V3–V4 region of the 16S rRNA gene and the partial *dsrAB* gene (using *Chlorobia*-targeted PCR primers 341f/GSB822r [72] and PGdsrAF/PGdsrAR [73], respectively). However, the appearances of cultures grown in ferrous iron-containing medium for these lakes differed from those of reference photoferrotrophic *Chlorobia* members. Instead of forming a reddish-brown ferric iron precipitate, the enrichments blackened, potentially indicative of sulfate reduction, and metal sulfide

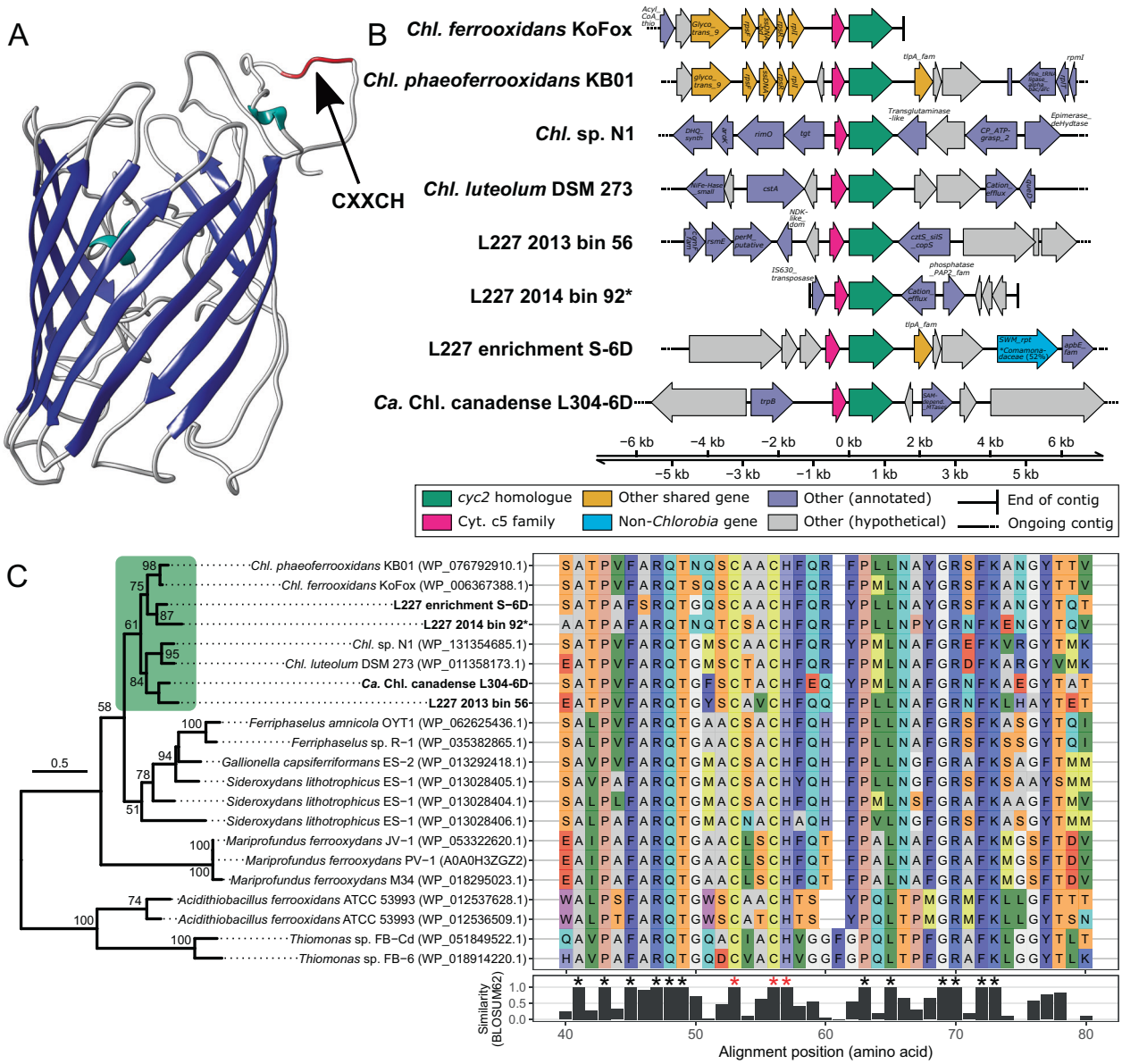

Fig. 1 Recovered *cyc2* homologs of *Chlorobia* from metagenomes. **a** Homology model of the Cyc2 protein from *Chl. phaeoferrooxidans* KB01, generated by I-TASSER based on sequence homology (with leading 18 signal peptides trimmed according to SignalP [88]) and visualized using UCSF Chimera [89]. The porin-like beta barrel structure is highlighted in dark blue, and the location of the single N-terminal heme-binding motif on the outer-membrane portion of the structure is indicated by a black arrow. **b** Genomic context of the recovered *cyc2* homologs. A ~10 kb region is shown of assembled contigs surrounding the homologs. The *cyc2* and adjacent *c5* family cytochrome genes are highlighted in green and pink, respectively. Other shared genes between contigs are highlighted in yellow. Remaining genes are colored gray if they lacked a functional annotation (e.g., no significant BLASTP hit, or hit to a domain of unknown function) or are colored purple if their closest BLASTP hit corresponded to a gene associated with the *Chlorobiaceae* family. One gene in the 10 kb region had its closest BLASTP hit to a gene associated with the *Comamonadaceae* family (*Betaproteobacteria*; ~51% amino acid identity); this gene is highlighted in blue. **c** Sequence comparison of recovered *cyc2* homologs to *cyc2* genes of known iron-oxidizing microorganisms. The phylogenetic tree was built from a 223 residue masked Cyc2 amino acid sequence alignment (see "Methods"). Bootstrap values over 50/100 are shown, and the scale bar represents the proportion of residue changes along the alignment. Due to the uncertain evolutionary history of *cyc2*, the phylogeny is midpoint rooted. A green box highlights the monophyletic *Chlorobia* clade. Adjacent to the phylogeny, a subset of the unmasked Cyc2 sequence alignment is shown (positions 40–80 of 609; N-terminus end). Alignment positions having 100% sequence identity in the predicted heme-binding site (CXXCH motif) are marked with red asterisks. Other positions with 100% sequence identity are marked with black asterisks. Note that L227 2014 Bin 92 (name marked with an asterisk) was included in this figure for comparison of its *cyc2* gene despite the bin quality being lower than the main *Chlorobia* genome bin set. *Chl. Chlorobium*.

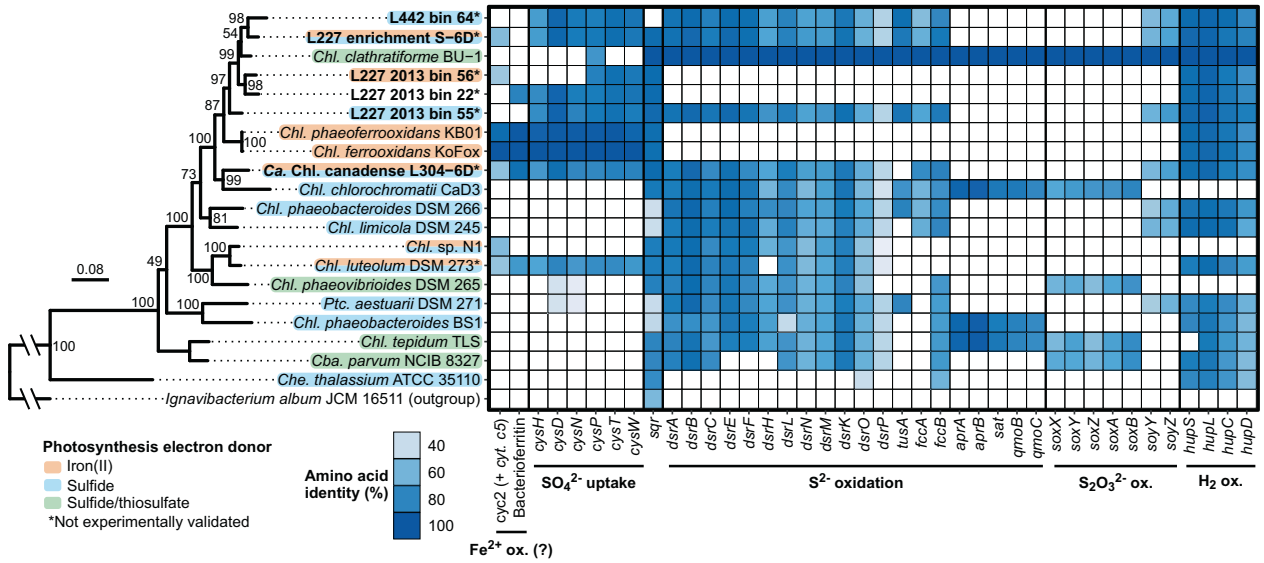

Fig. 2 Iron- and sulfur-oxidizing genetic potential in recovered genome bins of *Chlorobia* compared to reference strains. The left side of the figure shows a maximum-likelihood phylogenetic tree of the *Chlorobia* based on concatenated ribosomal protein amino acid sequences (see "Methods"). Bootstrap values over 50/100 are shown, and the scale bar represents the percentage of residue changes across the 2243 amino acid alignment. Species of *Chlorobia* are shaded based on their known or hypothesized metabolic potential. Genome bins of *Chlorobia* recovered from this study are bolded. On the right side, a heatmap is shown displaying the presence/absence of genes associated with iron and sulfur metabolism among *Chlorobia* based on bidirectional BLASTP. Heatmap tiles are shaded based on the percent amino acid identity of an identified gene compared to the reference sequence (*Chl. ferrooxidans* for putative iron metabolism-associated genes, and *Chl. phaeoclathratiforme* for sulfur metabolism-associated genes). Although the cytochrome *c5* family gene upstream of *cyc2* was not searched for directly due to poor sequence homology, the gene was verified manually to be adjacent to all hits of *cyc2*. *Chl. Chlorobium, Cba. Chlorobaculum, Che. Chloroherpeton, Ptc. Prosthecochloris*.

formation. After blackening, enrichments developed a green color (Supplementary Fig. 3). Suspecting that sulfate reduction was occurring in the ferrous iron enrichment bottles to support sulfide-oxidizing phototrophy, one Lake 227 enrichment was transferred into sulfide-containing media and still developed green pigmentation, albeit slowly (Supplementary Fig. 3). Amplification and Sanger sequencing of the partial *dsrAB* gene cluster from this enrichment showed that the gene sequence only differed by one ambiguous base from, and thus was essentially identical to, a corresponding Lake 227 sulfide enrichment. Ferrous iron enrichments eventually stopped being followed due to long growth times, low biomass, and instability of the cultures. Enrichments on sulfide-containing media were continued instead.

Metagenome sequencing of the two successful enrichments of *Chlorobia* grown on sulfide (L227 enrichment S-6D and L304 enrichment S-6D) showed that genome bins of the *Chlorobia* from both enrichments encoded *cyc2* homologs. Although L227 enrichment S-6D ceased to grow in laboratory culture, the L304 enrichment S-6D continued to be purified and was named "*Candidatus* Chlorobium canadense strain L304-6D". At the time of running the ferrous iron oxidation test (below), the "*Ca*. Chl. canadense" culture consisted of >90% cells of *Chlorobia* based on epifluorescence microscopy (Supplementary Fig. 4), and other contaminating cells were known to be chemoorganoheterotrophs and sulfate-reducing bacteria based on previous 16S rRNA gene amplicon sequencing data (Supplementary File 5).

Metabolic diversity and phylogeny of *Chlorobium* genome bins

Recovered genome bins of *Chlorobia* were genetically diverse with respect to the surveyed photosynthesis-associated genes (Fig. 2). One of the lake-recovered bins (L227 2013 Bin 56) lacked all assessed genes involved in sulfide, elemental sulfur, and thiosulfate oxidation but contained the *cyc2* gene homolog. Conversely, two other lake-recovered bins (L227 2013 Bin 55 and L442 Bin 64) contained all assessed genes in the sulfide oxidation pathway but lacked the *cyc2* gene. Although the final lake-recovered bin (L227 2013 Bin 22) lacked both *cyc2* and genes for sulfur oxidation, this lack of key metabolism genes might be due to incomplete genome binning. Lastly, the two enrichment culture bins encoded both *cyc2* and the sulfide oxidation gene pathway, similarly to *Chl.* sp. N1 and *Chl. luteolum*. Like some cultured photoferrotrophs, L227 2013 Bin 22 and the "*Ca*. Chl. canadense" genome also encoded putative homologs to a bacterioferritin hypothesized by Frigaard and Bryant [18] to play a role in photoferrotrophy. Genes for hydrogen oxidation were

detected in all of the genome bins (Fig. 2), along with marker genes for photosynthesis and bacteriochlorophyll biosynthesis (Supplementary Fig. 5). Marker genes for carbon fixation (via the reverse TCA cycle) were detected in all genome bins, with the exception of L227 2013 Bin 56, which was missing one of the two assessed gene clusters for the process (*aclAB*; Supplementary Fig. 5). Although L227 2013 Bin 56 was also missing half of the *cys* gene pathway for sulfate uptake (Fig. 2), the *cys* gene cluster occurred at the very end of a contig for this genome bin, implying that the bin likely ought to contain the complete *cys* pathway but that an assembly break occurred.

Phylogenetic analysis of the recovered *Chlorobium* genome bins based on concatenated ribosomal protein sequences showed that all four lake-recovered bins and the bin from the Lake 227 enrichment formed a monophyletic subgroup within the *Chlorobiaceae*, including *Chl. phaeoclathratiforme* BU-1 (Fig. 2). Directly basal to this subgroup was a branch containing *Chl. ferrooxidans* and *Chl. phaeoferrooxidans*. By comparison, the bin of "*Ca*. Chl. canadense" grouped sister to *Chl. chlorochromatii*, separately from the above group and from the group containing *Chl. luteolum* and *Chl*. sp. strain N1. Comparison of the concatenated ribosomal protein phylogeny to the *cyc2* predicted primary sequence phylogeny reveals some congruency between the two phylogenies for potentially photoferrotrophic members of the *Chlorobia*, with the exception of L227-S-6D and "*Ca*. Chl. canadense" (Supplementary Fig. 6). Overall, all six recovered *Chlorobium* genome bins appear to represent novel species, having an ANI of <79.6% compared to the genomes of all available type strains (Supplementary Fig. 1).

Functional and taxonomic profiling

Read mapping to genome bins showed that several distinct populations of *Chlorobia* were relevant to the lake environment (Fig. 3). Bins containing *cyc2* (no *dsrA*) and bins containing *dsrA* (no *cyc2*) were both found at similar relative abundances in Lake 227 samples in 2013 and 2014 (Fig. 3a). Generally, genome bins of *Chlorobia* containing *cyc2* accounted for 0.6–2.8% of the Lake 227 microbial community data in the assessed samples, whereas bins of *Chlorobia* containing *dsrA* accounted for 1.7–4.1% of the data. Analyses of unassembled metagenome read data indicated similar relative abundances (Supplementary Fig. 7). In contrast, only genome bins encoding sulfide oxidation were detected in Lake 442 metagenome assemblies. Even when unassembled metagenome data were scanned, only a single HMM hit from the Lake 442 metagenomes matched *cyc2* classified as belonging to a member of *Chlorobia*, compared to 27,000–37,000 total *rpoB* hits for these same metagenomes, showing that the lack of *cyc2* genes detected in genome bins of *Chlorobia* from L442 was not a result of incomplete assembly or genome binning. One genome bin of *Chlorobia* overlapped between L227 and L442 (L442 2011 16.5 m Bin 8); the rest were distinct between the two lakes. In addition, the bins of *Chlorobia* recovered from the enrichment culture metagenomes were not detected at high relative abundances in any of the six lake metagenomes.

Several non-*Chlorobia* genome bins were also found to contain the *cyc2* or *dsrA* gene through sequence searches (Fig. 3b). Genome bins containing potential *cyc2* homologs grouped into the *Rhodoferax* or *Gallionella* genera known to include iron-cycling bacteria [23, 74] or into the *Steroidobacteraceae* or *Methylomonadaceae* families. Given that both genomes associated with the *Steroidobacteraceae* (L442 Bin 75 and L442 Bin 84) also encoded the PCC-type *mtrABC* operon implicated in iron reduction (Supplementary Fig. 8) [21], it is possible that these genomes represent novel, neutrophilic iron-reducing bacterial populations related to the acidophile *Acidibacter ferrireducens*, for which genome sequencing data are not yet available [75]. The genome bins classified to the *Methylomonadaceae* occurred at high relative abundances in the lake metagenomes, having a cumulative relative abundance of up to ~17% in Lake 227 (Fig. 3c), and encoded particulate methane monooxygenase (*pmoA*) genes, with the exception of L442 2011 16.5 m Bin 5. These genome bins encoded a "repCluster2" *cyc2* variant based on analysis by FeGenie, unlike the "repCluster1" variants detected in genomes of *Chlorobia* and of *Gallionella*, but they encoded no detectable *cyc1* gene adjacent to the *cyc2* sequences as seen in the "repCluster2" *cyc2* sequences of *Rhodoferax* (Supplementary Fig. 8). Three other genome bins belonging to the phyla *Myxococcota* and *Verrucomicrobiota* encoded PCC-type gene clusters potentially involved in extracellular electron transfer (Supplementary Fig. 8). Several genomes, including all detected genomes of *Chlorobium*, were found based on FeGenie to encode a "repCluster3" *cyc2* variant (Supplementary Fig. 8). This distant homolog of the photoferrotrophy-associated "repCluster1" *cyc2* variant (having ~20% amino acid identity to "repCluster1" sequences) could potentially play a role in extracellular electron transfer but has not been associated with photoferrotrophy in reference cultures and was not detected by the custom HMM developed in this study.

Genome bins encoding *dsrA*, which is involved in either sulfide oxidation or sulfate reduction, included a bin related to known chemolithotrophic sulfide-oxidizing bacteria of the genus *Sulfuritalea* and a bin related to heterotrophic sulfate-reducing bacteria of the family *Desulfatirhabdiaceae* [76, 77]. A bin classified to the family *Smithellaceae* of the order *Syntrophales*, along with a bin classified to the genus *Rhodoferax*, also encoded *dsrA*. Three of these four genomes bins were also found to encode the *aprAB* operon

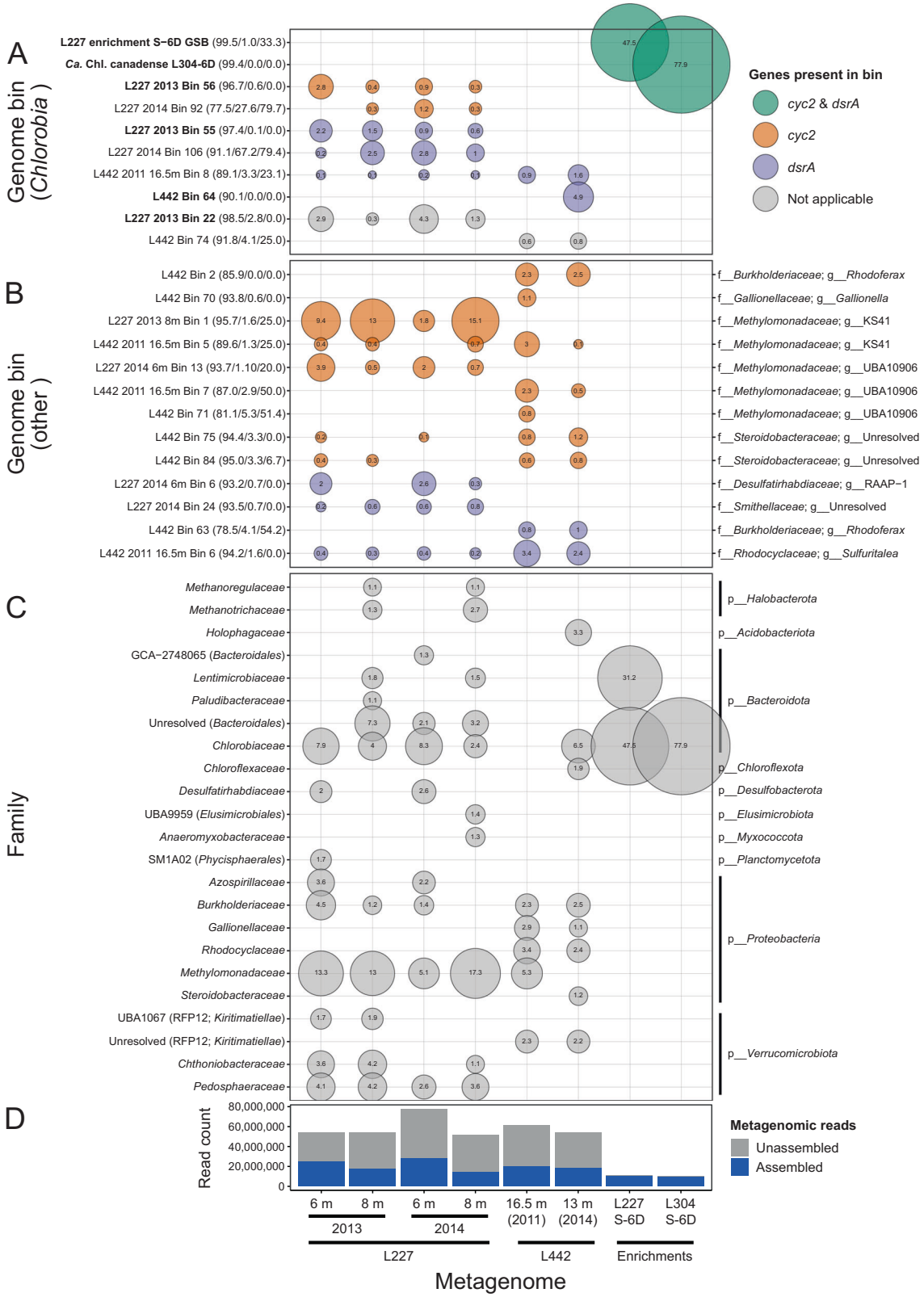

involved in sulfite metabolism (Supplementary Fig. 8). The two bins related to the *Sulfuritalea* and *Rhodoferax* genera were found to encode the *soxB* gene involved in thiosulfate oxidation (Supplementary Fig. 8), which suggests that both genome bins can oxidize sulfur compounds [18]. No other genome bins in the dataset were found to encode these key

Fig. 3 Bubble plot showing predicted relative abundances of recovered genome bins in the lake and enrichment culture metagenomes. The size of each bubble corresponds to the relative abundance of a genome bin or taxon within metagenome data based on mapping of assembled reads. Each bubble is also labeled with its percent relative abundance for clarity. **a** Bins of *Chlorobia* colored by their metabolic potential based on functional gene markers described in this study. Bolded names correspond to the higher-quality bins described in Table 1 and Fig. 2. In parentheses beside each name are bin quality statistics reported by CheckM—the predicted % completion, % contamination, and % strain heterogeneity, respectively. The displayed bins all classify to the *Chlorobium* genus based on GTDB taxonomy. **b** Non-*Chlorobia* bins (≥0.01% relative abundance) found to have the same functional gene markers (*cyc2* or *dsrA*) in their genome sequences. Quality statistics are reported as in **a**. On the right side of the panel, the GTDB family and genus classifications of each bin are shown. **c** Family-level taxonomic composition of the metagenomes based on GTDB classifications of genome bins with ≥1% relative abundance. The phylum of each family is displayed on the right side of the panel. For unresolved or non-Latin family names, the order (and class, if needed) is displayed in parentheses beside the family name for clarity. **d** Assembly statistics for the metagenome data. The total number of quality-trimmed metagenome reads is represented by the total height of each bar. Reads that mapped to the filtered sequence assembly (i.e., excluding short contigs, see "Methods") are highlighted in blue and are considered "assembled" reads. Assembled read totals were used to determine relative abundances of genome bins in **a**–**c**. Supplementary Figure 7 shows relative abundances based on predictions from unassembled metagenome reads for comparison.

sulfur-cycling gene markers except for two genome bins that could not be confidently classified as sulfur cyclers due to limited gene content (Supplementary Fig. 8).

Chlorobia members appeared to represent the dominant phototrophs in the lake anoxic zone samples. In total, genome bins classified to the *Chlorobia* represented as high as 8.3% of lake microbial communities based on read mapping (Fig. 3c). Predicted relative abundances of populations of *Chlorobia* were 1.2–1.8 times higher when unassembled reads were assessed directly (Supplementary Fig. 7), with a predicted maximum relative abundance of 12.3%, showing that high relative abundance is not a result of assembly bias (Fig. 3d). The only other potential chlorophototroph detected in the dataset at >1% relative abundance was a single genome bin classified to the family *Chloroflexaceae* (L442 Bin 82; 92.9/1.2% completeness/contamination), which made up 1.9% of the L442 microbial community in 2014 at 15 m depth (Fig. 3c) and contained the *bchL* and *pufM* photosynthesis genes (data not shown). This genome bin was undetected in all other samples.

Assessment of ferrous iron oxidation potential of "*Ca*. Chl. canadense"

Cultures of *Chl. ferrooxidans* showed the expected behavior when incubated in ferrous iron containing medium. After a short lag phase, both *Chl. ferrooxidans* cultures containing 100 µM $FeCl_2$ (no EDTA) and exposed to light began oxidizing ferrous iron, and the cultures had nearly completely oxidized all ferrous iron within 2 days of the initial setup (Fig. 4). Similar bottles incubated in the dark showed consistent iron oxidation rates of ~5 µM d^{-1} that corresponded to rates observed in uninoculated media controls; this iron oxidation was inferred to be abiotic, for example due to small amounts of oxygen contamination during sampling. No ferrous iron oxidation outside of this baseline effect was observed in the *Chl. ferrooxidans* cultures supplemented with 120 µM EDTA, in contrast to the stimulatory effect of EDTA reported for *Rhodopseudomonas palustris* TIE-1 [68], which uses a different gene system (*pioAB*) for extracellular electron transfer [24]. The EDTA-amended medium consistently appeared to have ~50% ferrous iron oxidation at the beginning of the experiment, based on the ferrozine assay, but this apparent oxidation has been observed previously with EDTA and could potentially be due to ineffective binding of ferrozine to EDTA-chelated iron [70].

In contrast to *Chl. ferrooxidans*, "*Ca*. Chl. canadense" showed no photoferrotrophic iron oxidation activity over the course of the experiment (Fig. 4; Supplementary Fig. 9), and the iron oxidation profiles of the cultures closely matched those of the uninoculated media control bottles. A reference bottle of Hegler freshwater medium prepared in the same batch as those in the main experiment but amended with 600 µM buffered sulfide feeding solution, in place of ferrous iron, received the same inoculum of "*Ca*. Chl. canadense". Complete oxidation of sulfide in the bottle was observed within 5 days of inoculation and incubation under light (not shown), indicating that the media and inoculum were not the cause of the lack of observed photoferrotrophic activity.

Discussion

In this study, we explored the diversity of anoxygenic photosynthesis in the ferruginous water columns of Boreal Shield lakes and evaluated the potential for photoferrotrophy using a combination of genome-resolved metagenomics and enrichment cultivation. Although we were unable to induce photoferrotrophy in laboratory cultures, we detected robust homologs of the *cyc2* gene associated with photoferrotrophy in the genus *Chlorobium* and found evidence for both iron cycling and cryptic sulfur cycling in the lakes. Overall, our findings provide genomic context to previous 16S rRNA gene data supporting the existence of *Chlorobia*-driven photoferrotrophy in Boreal Shield lakes [4], adding nuance to the interpretation of these data while expanding sparse knowledge of the diversity of *cyc2* within the *Chlorobia*. Our research reinforces the need for additional genetic work to understand the function and regulation of *cyc2* in photoferrotrophy.

We detected several novel variants of *cyc2* in the genome bins of *Chlorobia* recovered in this study from lake and

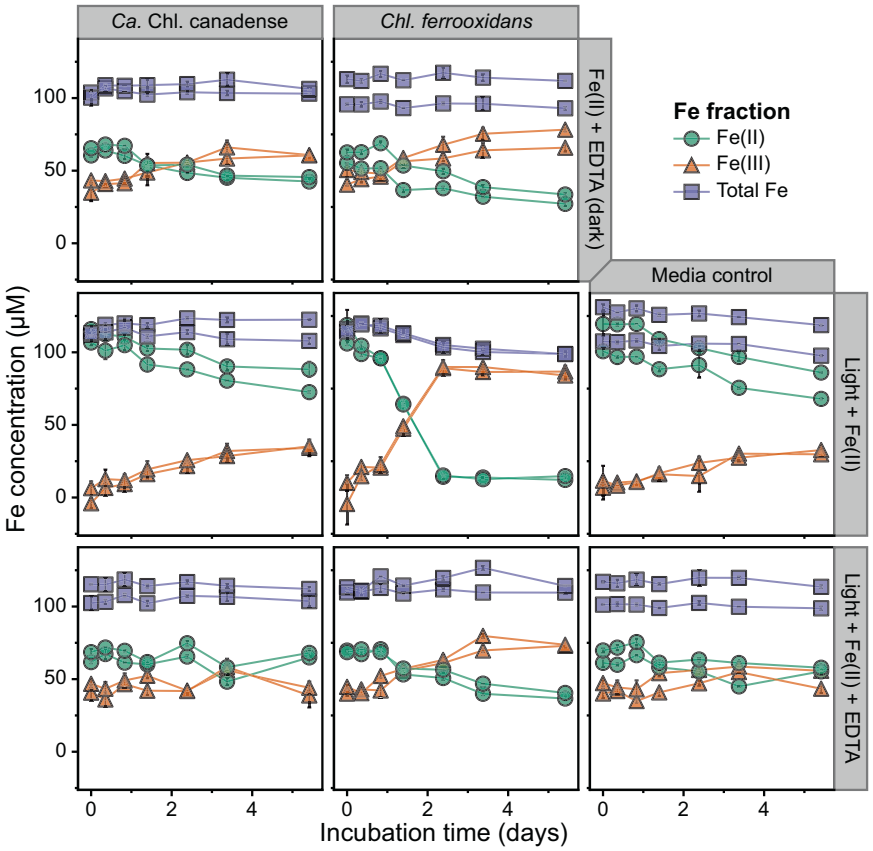

Fig. 4 Iron oxidation activity of two *Chlorobia* cultures under different growth conditions over time. The concentrations of ferrous iron, total iron, and ferric iron (determined by the subtraction of ferrous iron from total iron) are shown over a 10 day incubation period for "*Ca.* Chl. canadense" (enriched in this study) and *Chl. ferrooxidans*. The activity of the cultures in iron-amended media is shown when incubated in the dark with EDTA, in the light, and in the light with EDTA. Each panel depicts the results of biological duplicates, with error bars representing the standard deviation of technical duplicates in the ferrozine assay. The same results are shown for the full 21-day incubation period in Supplementary Fig. 9.

enrichment culture metagenomes (Fig. 1). The *cyc2* gene, which is putatively implicated in ferrous iron oxidation among microaerophilic iron-oxidizing bacteria [27], has been hypothesized to play a role in photoferrotrophy based on its presence in the genomes of cultured photoferrotrophs within the *Chlorobia* and its absence in the genomes of strict sulfide-oxidizing *Chlorobia* members. Our detection of four additional high-confidence homologs of *cyc2* doubles the known diversity of this gene among members of the *Chlorobia* compared to cultured representatives, and we also developed a robust method combining sequence composition, genomic context, and phylogenetic placement for detection of additional *cyc2* homologs compared to related cytochromes. Our work suggests that *cyc2*-encoding *Chlorobia* members, although only cultivated in the laboratory recently, play an important role in seasonally anoxic Boreal Shield lake microbial communities based on their high relative abundances in lake metagenomes (Fig. 3a).

Homologs of *cyc2* also appear to be associated with other bacteria potentially involved in iron cycling in Lakes 227 and 442. One genome bin classified to the genus *Gallionella*, L442 Bin 70, encoded *cyc2*, and could represent a microaerophilic iron-oxidizing bacterium. In addition, genomes such as L442 Bin 2 classified to the genus *Rhodoferax* (related to *Rhodoferax ferrireducens*) and L442 Bins 75 and 84 belonging to the *Steroidobacteraceae* (related to *Acidibacter ferrireducens*) encoded an alternative *cyc1/cyc2* gene cluster and could correspond to known iron-reducing bacteria. Other bacterial genomes encoding PCC-type gene systems involved in extracellular electron transfer were also detected, hinting at a broader iron-based biogeochemical cycle in the lakes. At the same time, genome bins classified to the *Methylomonadaceae* that are unrelated to known iron-cycling bacteria also encoded an alternative *cyc2* variant. It is possible that the *cyc2* variant might be involved in a form of extracellular electron transfer for these potential methanotrophs, which are found in the anoxic zones of Lakes 227 and 442 despite the oxygen requirement for particulate methane monooxygenase, as recently observed for other lakes [78, 79]. However, extracellular electron transfer by bacterial methanotrophs has not been reported in the literature previously, leaving the role of these *cyc2* homologs unclear. Altogether, our data suggest that iron metabolism plays an important biogeochemical role in the seasonally anoxic and ferruginous water columns of these lakes.

Along with *cyc2*, we also detected genomic potential for sulfide oxidation among genome bins of *Chlorobia* recovered in this study. A higher number of genome bins of *Chlorobia* encoded the genetic potential for sulfide oxidation (based on the marker gene *dsrA*) than encoded *cyc2*, and in addition, *cyc2* associated with *Chlorobia* members was entirely undetectable in Lake 442 metagenome data.

Combined with our observations of blackening of ferrous iron-containing medium during initial enrichment culturing before phototrophic growth (Supplementary Fig. 3), our data suggest that sulfide is an important electron donor for anoxygenic phototrophs in ferruginous Boreal Shield lake waters. We detected at least one genome bin at high relative abundance in Lake 227 that likely represented a sulfate-reducing bacterium (Fig. 3c; Supplementary Fig. 8) and might thus provide the required sulfide to sustain phototrophic sulfide oxidation, even if sulfide is at low levels overall in the lakes. Such "cryptic sulfur cycling", where sulfur turnover is rapid at low measured concentrations of sulfur redox species, has been observed previously in other sulfide-limited systems [80], including the permanently anoxic and ferruginous Lake La Cruz [81], and might have also played an important role in Archaean oceans once sufficient organic carbon was available. In addition, because all detected genomes of *Chlorobia* encoded the *hupLS* genes (Fig. 2), it is possible that oxidation of molecular hydrogen, as observed in laboratory cultures of *Chlorobia* [14], could also play a role in the metabolism of the populations of *Chlorobia* in the lakes.

We were unable to induce photoferrotrophy in "*Ca*. Chl. canadense" (Fig. 4), which we enriched in a sulfide-containing medium, despite the fact that this organism encoded a *cyc2* homolog and a bacterioferritin in its genome (Fig. 2). The lack of observed photoferrotrophic growth in "*Ca*. Chl. canadense" could be due to several reasons. Firstly, it is possible that, although *cyc2* is associated with reference photoferrotrophic *Chlorobia* members, the *cyc2* gene plays a peripheral role in the metabolism of these organisms and is not directly involved in photoferrotrophy. Secondly, *cyc2* could represent a single step in a larger iron oxidation gene pathway that is missing in the "*Ca*. Chl. canadense" genome. For example, the *c5* family cytochrome detected directly upstream of all *cyc2* homologs identified among genomes of *Chlorobia* (Fig. 1b) could potentially be involved in iron electron transfer. Unlike the primary sequences of all other *c5* family cytochromes adjacent to *cyc2* in reference genomes or environmental genome bins, the *c5* family cytochrome of "*Ca*. Chl. canadense" contains an additional cysteine residue in the heme-binding motif in its primary sequence (i.e., CCXCH rather than the typical CXXCH; Supplementary Fig. 2) that could have deleterious consequences for iron oxidation [82].

As a third possibility, *cyc2* could be associated with alternative cellular roles, including electron exchange with humic substances as hypothesized by He et al. [83] or even direct electron uptake from solid-phase conductive substances, as has been observed in the photoferrotroph *Rps. palustris* TIE-1 [84]. However, direct links between Cyc2 and oxidation of alternate substrates to dissolved ferrous iron have not been demonstrated experimentally. Lastly, the *cyc2* gene product in "*Ca*. Chl. canadense" might allow for iron oxidation but might not be readily expressed under our laboratory conditions. This option would align with preliminary reports that the *cyc2*-encoding but sulfide-oxidizing *Chl. luteolum* is capable of changing to photoferrotrophic growth (Kate Thompson and Sean Crowe, personal communication), despite previous difficulties inducing this behavior [16]. The "*Ca*. Chl. canadense" culture can be used to probe the regulation and function of *cyc2* within the class *Chlorobia* in future work, especially given its atypical cytochrome *c5* sequence and given that all other *cyc2*-encoding and cultured *Chlorobia* members to date have photoferrotrophic activity. However, we are unable to draw conclusive links between *cyc2* and photoferrotrophy from the present study.

Despite being physically nearby (~13.5 km apart) and having similar overall physico-chemistry, Lakes 227 and 442 differed substantially in the microbial community composition of their anoxic water columns based on metagenome data. Most genome bins examined in this study (Fig. 3a, b) were specific to one of the two lakes based on read mapping counts. Such single-lake specificity is lost when summarizing data at higher taxonomic levels (e.g., Fig. 3c) and was not observed for the same DNA samples when analyzed previously using 16S rRNA gene amplicon sequencing and clustering of sequences at a 97% identity threshold [4]. Our population-level analyses showed that *cyc2* was not encoded by Lake 442 genome bins of *Chlorobia* despite being encoded by genome bins of *Chlorobia* in Lake 227 metagenome data. It is possible that physicochemical differences between the lakes, such as ferrous iron and sulfate concentration, hydrogen and bicarbonate concentrations (observed to impact photoferrotrophy rates in *Rps. palustris* TIE-1 [85]), lake bathymetry, anoxia timing, pH, light quality, or dissolved organic carbon levels, could drive this and other microbial community differences between the two lakes. Understanding key factors governing the favourability of *cyc2* among Boreal Shield lakes could prove valuable for understanding the ecology and function of *cyc2*.

The strong iron isotope fractionation observed between the oxic and anoxic zone boundaries of Lakes 227 and 442 previously by Schiff et al. [4] appears to occur regardless of whether *Chlorobia*-affiliated *cyc2* genes are detectable. It is possible that microaerophilic iron oxidation could contribute to the observed iron isotope fractionation in Lake 442 given the detection of a *cyc2*-encoding genome bin within the *Gallionella* in Lake 442 metagenomic data (Fig. 3b). Partial iron reduction by iron-reducing bacteria might also contribute to the observed fractionation. However, other yet-unknown iron cycling processes might also be at work. Sampling for iron isotopes at higher spatial and temporal resolution, combined with knowledge of additional iron-cycling processes in the lakes, could allow for

the sources of the observed isotopic fractionation in both lakes to be determined, with implications for reconstructing ancient biogeochemical cycles from the rock record.

Our research provides insight into the metabolic diversity and ecology of anoxygenic photoautotrophs in seasonally anoxic Boreal Shield lakes. We show that high relative abundance genome bins of *Chlorobia* in lake metagenomes can encode the *cyc2* gene associated with iron oxidation but that phototrophic sulfide oxidation is more widespread and reproducible in the laboratory. Although we were unable to induce photoferrotrophic growth, we enriched the novel *cyc2*-encoding species "*Ca*. Chl. canadense", which could be used in future research exploring the function and regulation of *cyc2* as genetic studies continue to progress in linking the *cyc2* gene product to its cellular role [86]. Probing the metabolic diversity of anoxygenic phototrophs in Boreal Shield lakes could lead to novel inferences about photosynthesis in early Earth oceans, including the role of cryptic sulfur cycling compared to photoferrotrophic activity. Novel phototrophic metabolisms, such as recently reported phototrophic oxidation of manganese(II) [87], could also be explored with implications for both modern and prehistoric biogeochemical cycling. Altogether, our findings serve as an important basis for future work probing the biogeography and activity of anoxygenic phototrophs in natural waters. Understanding the metabolic diversity of phototrophy in Boreal Shield lakes will enhance our comprehension of modern boreal ecosystems with additional implications for the evolution of early life on Earth.

Data availability

Raw metagenome reads for the freshwater lake and enrichment culture metagenomes are available in the NCBI sequence read archive (SRA) under BioProjects PRJNA518727 and PRJNA534305, respectively. Six curated genome bins of *Chlorobia* are available under the same BioProjects, along with all assembled contigs from freshwater lake metagenomes. The complete set of uncurated genome bins were uploaded to a Zenodo repository at https://doi.org/10.5281/zenodo.2720705. Code for downloading these data and performing the analyses presented in this paper, along with intermediate data files, are available at https://github.com/jmtsuji/Chlorobia-cyc2-genomics (https://doi.org/10.5281/zenodo.3228523).

Acknowledgements We thank R. Henderson and staff at the IISD-ELA for assistance in field sampling and interpretation of the dynamics of ELA lakes. In addition, we thank S.A. Crowe for valuable feedback on the paper, K.J. Thompson for helpful discussion related to the work, L.H. Bergstrand for assistance with bioinformatics, and K.E. Engel, R.C. Beaver, and N.A. Shaw for assistance with laboratory tasks. JMT thanks M.S.M. Jetten, C.U. Welte, and staff at the Soehngen Institute of Anaerobic Microbiology, for providing helpful training for anaerobic microbiology methods. We also thank the editor and anonymous peer reviewers for helpful feedback that enhanced the quality and scope of this work. This research was supported by Discovery Grants and a Strategic Partnership Grant for Projects from the National Sciences and Engineering Research Council of Canada.

Author contributions SLS, JJV, and LM were involved in the overall lake sampling project that led to this work and provided input and assistance with sample collection and data interpretation. JMT and JDN designed the experimental work in this study. JMT, NT, and MT performed enrichment cultivation with support from SH. JMT analyzed the sequence data and drafted the paper with the edits and feedback of all authors.

Compliance with ethical standards

Conflict of interest The authors declare that they have no conflict of interest.

Publisher's note Springer Nature remains neutral with regard to jurisdictional claims in published maps and institutional affiliations.

References

1. Keller W. Implications of climate warming for Boreal Shield lakes: a review and synthesis. Environ Rev. 2007;15:99–112.
2. Teodoru CR, del Giorgio PA, Prairie YT, Camire M. Patterns in $p\ CO_2$ in boreal streams and rivers of northern Quebec, Canada. Glob Biogeochem Cycles. 2009;23:GB2012.
3. Anas MUM, Scott KA, Wissel B. Carbon budgets of boreal lakes: state of knowledge, challenges, and implications. Environ Rev. 2015;23:275–87.
4. Schiff SL, Tsuji JM, Wu L, Venkiteswaran JJ, Molot LA, Elgood RJ, et al. Millions of Boreal Shield lakes can be used to probe Archaean Ocean biogeochemistry. Sci Rep. 2017;7:46708.
5. Poulton SW, Canfield DE. Ferruginous conditions: a dominant feature of the ocean through Earth's history. Elements. 2011;7:107–12.
6. Parks DH, Chuvochina M, Waite DW, Rinke C, Skarshewski A, Chaumeil P-A, et al. A standardized bacterial taxonomy based on genome phylogeny substantially revises the tree of life. Nat Biotechnol. 2018;36:996–1004.
7. Karhunen J, Arvola L, Peura S, Tiirola M. Green sulphur bacteria as a component of the photosynthetic plankton community in small dimictic humic lakes with an anoxic hypolimnion. Aquat Microb Ecol. 2013;68:267–72.
8. Imhoff JF. The family *Chromatiaceae*. In: Rosenberg E, DeLong EF, Lory S, Stackebrandt E, Thompson F, editors. The Prokaryotes. Berlin Heidelberg: Springer; 2014. pp. 151–78.
9. Imhoff JF. The family *Chlorobiaceae*. In: Rosenberg E, DeLong EF, Lory S, Stackebrandt E, Thompson F, editors. The Prokaryotes. Berlin Heidelberg: Springer; 2014. pp. 501–14.
10. Ehrenreich A, Widdel F. Anaerobic oxidation of ferrous iron by purple bacteria, a new type of phototrophic metabolism. Appl Environ Microbiol. 1994;60:4517–26.
11. Griffin BM, Schott J, Schink B. Nitrite, an electron donor for anoxygenic photosynthesis. Science. 2007;316:1870.
12. Kulp TR, Hoeft SE, Asao M, Madigan MT, Hollibaugh JT, Fisher JC, et al. Arsenic(III) fuels anoxygenic photosynthesis in hot spring biofilms from Mono Lake, California. Science. 2008;321:967–70.

13. Thiel V, Tank M, Bryant DA. Diversity of chlorophototrophic bacteria revealed in the omics era. Annu Rev Plant Biol. 2018;69: 21–49.
14. Heising S, Richter L, Ludwig W, Schink B. *Chlorobium ferrooxidans* sp. nov., a phototrophic green sulfur bacterium that oxidizes ferrous iron in coculture with a "*Geospirillum*" sp. strain. Arch Microbiol. 1999;172:116–24.
15. Llirós M, García–Armisen T, Darchambeau F, Morana C, Triadó–Margarit X, Inceoğlu Ö, et al. Pelagic photoferrotrophy and iron cycling in a modern ferruginous basin. Sci Rep. 2015;5:13803.
16. Laufer K, Niemeyer A, Nikeleit V, Halama M, Byrne JM, Kappler A. Physiological characterization of a halotolerant anoxygenic phototrophic Fe(II)-oxidizing green-sulfur bacterium isolated from a marine sediment. FEMS Microbiol Ecol. 2017;93:fix054.
17. Lambrecht N. Insights into early Earth ocean biogeochemistry from intensive monitoring of two ferruginous meromictic lakes. PhD thesis. Iowa, USA:Iowa State University;2019.
18. Frigaard N-U, Bryant DA. Genomic insights into the sulfur metabolism of phototrophic green sulfur bacteria. In: Hell R, Dahl DC, Knaff D, Leustek T, editors. Sulfur metabolism in phototrophic organisms. Netherlands: Springer; 2008. pp. 337–55.
19. Camacho A, Walter XA, Picazo A, Zopfi J. Photoferrotrophy: remains of an ancient photosynthesis in modern environments. Front Microbiol. 2017;8:323.
20. Koeksoy E, Halama M, Konhauser KO, Kappler A. Using modern ferruginous habitats to interpret Precambrian banded iron formation deposition. Int J Astrobiol. 2016;15:205–17.
21. He S, Barco RA, Emerson D, Roden EE. Comparative genomic analysis of neutrophilic iron(II) oxidizer genomes for candidate genes in extracellular electron transfer. Front Microbiol. 2017;8:1584.
22. Melton ED, Swanner ED, Behrens S, Schmidt C, Kappler A. The interplay of microbially mediated and abiotic reactions in the biogeochemical Fe cycle. Nat Rev Microbiol. 2014;12:797–808.
23. Kato S, Ohkuma M, Powell DH, Krepski ST, Oshima K, Hattori M, et al. Comparative genomic insights into ecophysiology of neutrophilic, microaerophilic iron oxidizing bacteria. Front Microbiol. 2015;6:1265.
24. Gupta D, Sutherland MC, Rengasamy K, Meacham JM, Kranz RG, Bose A. Photoferrotrophs produce a PioAB electron conduit for extracellular electron uptake. mBio. 2019;10:e02668–19.
25. Castelle C, Guiral M, Malarte G, Ledgham F, Leroy G, Brugna M, et al. A new iron-oxidizing/O_2-reducing supercomplex spanning both inner and outer membranes, isolated from the extreme acidophile Acidithiobacillus ferrooxidans. J Biol Chem. 2008;283:25803–11.
26. Barco RA, Emerson D, Sylvan JB, Orcutt BN, Meyers MEJ, Ramírez GA, et al. New insight into microbial iron oxidation as revealed by the proteomic profile of an obligate iron-oxidizing chemolithoautotroph. Appl Environ Microbiol. 2015;81:5927–37.
27. McAllister SM, Polson SW, Butterfield DA, Glazer BT, Sylvan JB, Chan CS. Validating the Cyc2 neutrophilic iron oxidation pathway using meta-omics of Zetaproteobacteria iron mats at marine hydrothermal vents. mSystems. 2020;5:e00553–19.
28. Crowe SA, Hahn AS, Morgan-Lang C, Thompson KJ, Simister RL, Llirós M, et al. Draft genome sequence of the pelagic photoferrotroph *Chlorobium phaeoferrooxidans*. Genome Announc. 2017;5:e01584–16.
29. Thompson KJ, Simister RL, Hahn AS, Hallam SJ, Crowe SA. Nutrient acquisition and the metabolic potential of photoferrotrophic Chlorobi. Front Microbiol. 2017;8:1212.
30. Bryce C, Blackwell N, Straub D, Kleindienst S, Kappler A. Draft genome sequence of *Chlorobium* sp. strain N1, a marine Fe(II)-oxidizing green sulfur bacterium. Microbiol Resour Announc. 2019;8:e00080–19.
31. Schindler DW, Armstrong FAJ, Holmgren SK, Brunskill GJ. Eutrophication of Lake 227, Experimental Lakes Area, northwestern Ontario, by addition of phosphate and nitrate. J Fish Res Board Can. 1971;28:1763–82.
32. Campbell P. Phosphorus budgets and stoichiometry during the open-water season in two unmanipulated lakes in the Experimental Lakes Area, northwestern Ontario. Can J Fish Aquat Sci. 1994;51:2739–55.
33. White RA III, Brown J, Colby S, Overall CC, Lee J-Y, Zucker J, et al. ATLAS (Automatic Tool for Local Assembly Structures) - a comprehensive infrastructure for assembly, annotation, and genomic binning of metagenomic and metatranscriptomic data. PeerJ Prepr. 2017;5:e2843v1.
34. Kieser S, Brown J, Zdobnov EM, Trajkovski M, McCue LA. ATLAS: a Snakemake workflow for assembly, annotation, and genomic binning of metagenome sequence data. BMC Bioinform. 2020;21:257.
35. Jeans C, Singer SW, Chan CS, VerBerkmoes NC, Shah M, Hettich RL, et al. Cytochrome 572 is a conspicuous membrane protein with iron oxidation activity purified directly from a natural acidophilic microbial community. ISME J. 2008;2:542–50.
36. Sievers F, Wilm A, Dineen D, Gibson TJ, Karplus K, Li W, et al. Fast, scalable generation of high-quality protein multiple sequence alignments using Clustal Omega. Mol Syst Biol. 2011;7:539.
37. Eddy SR. Accelerated profile HMM searches. PLOS Comput Biol. 2011;7:e1002195.
38. Talavera G, Castresana J. Improvement of phylogenies after removing divergent and ambiguously aligned blocks from protein sequence alignments. Syst Biol. 2007;56:564–77.
39. Nguyen L-T, Schmidt HA, von Haeseler A, Minh BQ. IQ-TREE: a fast and effective stochastic algorithm for estimating maximum-likelihood phylogenies. Mol Biol Evol. 2015;32:268–74.
40. Kalyaanamoorthy S, Minh BQ, Wong TKF, von Haeseler A, Jermiin LS. ModelFinder: fast model selection for accurate phylogenetic estimates. Nat Methods. 2017;14:587–9.
41. Olm MR, Brown CT, Brooks B, Banfield JF. dRep: a tool for fast and accurate genomic comparisons that enables improved genome recovery from metagenomes through de-replication. ISME J. 2017;11:2864–8.
42. Parks DH, Imelfort M, Skennerton CT, Hugenholtz P, Tyson GW. CheckM: assessing the quality of microbial genomes recovered from isolates, single cells, and metagenomes. Genome Res. 2015;25:1043–55.
43. Eren AM, Esen ÖC, Quince C, Vineis JH, Morrison HG, Sogin ML, et al. Anvi'o: an advanced analysis and visualization platform for 'omics data. PeerJ. 2015;3:e1319.
44. Rissman AI, Mau B, Biehl BS, Darling AE, Glasner JD, Perna NT. Reordering contigs of draft genomes using the Mauve Aligner. Bioinformatics. 2009;25:2071–3.
45. Seemann T. Prokka: rapid prokaryotic genome annotation. Bioinformatics. 2014;30:2068–9.
46. Armstrong FAJ, Schindler DW. Preliminary chemical characterization of waters in the Experimental Lakes Area, northwestern Ontario. J Fish Res Board Can. 1971;28:171–87.
47. Schindler DW. Eutrophication and recovery in experimental lakes: implications for lake management. Science. 1974;184:897–9.
48. Schindler D. The coupling of elemental cycles by organisms: evidence from whole-lake chemical perturbations. In: Stumm W, editor. Chemical processes in lakes. New York, NY: John Wiley and Sons; 1985. pp. 225–250.
49. Schindler DW. The dilemma of controlling cultural eutrophication of lakes. Proc R Soc B Biol Sci. 2012;279:4322–33.
50. Curtis PJ, Schindler DW. Hydrologic control of dissolved organic matter in low-order Precambrian Shield lakes. Biogeochemistry. 1997;36:125–38.
51. Hegler F, Posth NR, Jiang J, Kappler A. Physiology of phototrophic iron(II)-oxidizing bacteria: implications for modern and ancient environments. FEMS Microbiol Ecol. 2008;66:250–60.

52. Milucka J, Kirf M, Lu L, Krupke A, Lam P, Littmann S, et al. Methane oxidation coupled to oxygenic photosynthesis in anoxic waters. ISME J. 2015;9:1991–2002.
53. Clavier CGJ, Boucher G. The use of photosynthesis inhibitor (DCMU) for in situ metabolic and primary production studies on soft bottom benthos. Hydrobiologia. 1992;246:141–5.
54. Jain C, Rodriguez-R LM, Phillippy AM, Konstantinidis KT, Aluru S. High throughput ANI analysis of 90K prokaryotic genomes reveals clear species boundaries. Nat Commun. 2018;9:5114.
55. Lee MD. GToTree: a user-friendly workflow for phylogenomics. Bioinformatics. 2019;35:4162–4.
56. Hug LA, Baker BJ, Anantharaman K, Brown CT, Probst AJ, Castelle CJ, et al. A new view of the tree of life. Nat Microbiol. 2016;1:16048.
57. Altschul SF, Gish W, Miller W, Myers EW, Lipman DJ. Basic local alignment search tool. J Mol Biol. 1990;215:403–10.
58. Bergstrand LH, Cardenas E, Holert J, Hamme JDV, Mohn WW. Delineation of steroid-degrading microorganisms through comparative genomic analysis. mBio. 2016;7:e00166–16.
59. Bryant DA, Liu Z, Li T, Zhao F, Costas AMG, Klatt CG, et al. Comparative and functional genomics of anoxygenic green bacteria from the taxa *Chlorobi*, *Chloroflexi*, and *Acidobacteria*. In: Burnap R, Vermaas W, editors. Functional genomics and evolution of photosynthetic systems. Netherlands, Dordrecht: Springer; 2012. pp. 47–102.
60. Tourova TP, Kovaleva OL, Gorlenko VM, Ivanovsky RN. Use of genes of carbon metabolism enzymes as molecular markers of Chlorobi phylum representatives. Microbiology. 2013;82:784–93.
61. Chaumeil P-A, Mussig AJ, Hugenholtz P, Parks DH. GTDB-Tk: a toolkit to classify genomes with the Genome Taxonomy Database. Bioinformatics. 2020;36:1925–7.
62. Fish JA, Chai B, Wang Q, Sun Y, Brown CT, Tiedje JM, et al. FunGene: the functional gene pipeline and repository. Front Microbiol. 2013;4:291.
63. Hyatt D, Chen G-L, LoCascio PF, Land ML, Larimer FW, Hauser LJ. Prodigal: prokaryotic gene recognition and translation initiation site identification. BMC Bioinform. 2010;11:1–11.
64. Petrenko P, Lobb B, Kurtz DA, Neufeld JD, Doxey AC. MetAnnotate: function-specific taxonomic profiling and comparison of metagenomes. BMC Biol. 2015;13:1–8.
65. Garber AI, Nealson KH, Okamoto A, McAllister SM, Chan CS, Barco RA, et al. FeGenie: a comprehensive tool for the identification of iron genes and iron gene neighborhoods in genome and metagenome assemblies. Front Microbiol. 2020;11:37.
66. Pfennig N. *Rhodocyclus purpureus* gen. nov. and sp. nov., a ring-shaped, vitamin B_{12}-requiring member of the family *Rhodospirillaceae*. Int J Syst Evol Microbiol. 1978;28:283–8.
67. Tank M, Bryant DA. Nutrient requirements and growth physiology of the photoheterotrophic Acidobacterium, *Chloracidobacterium thermophilum*. Front Microbiol. 2015;6:226.
68. Peng C, Bryce C, Sundman A, Borch T, Kappler A. Organic matter complexation promotes Fe(II) oxidation by the photoautotrophic Fe(II)-oxidizer *Rhodopseudomonas* palustris TIE-1. ACS Earth Space Chem. 2019;3:531–6.
69. Stookey LL. Ferrozine—a new spectrophotometric reagent for iron. Anal Chem. 1970;42:779–81.
70. Verschoor MJ, Molot LA. A comparison of three colorimetric methods of ferrous and total reactive iron measurement in freshwaters. Limnol Oceanogr Methods. 2013;11:113–25.
71. Yang J, Yan R, Roy A, Xu D, Poisson J, Zhang Y. The I-TASSER Suite: protein structure and function prediction. Nat Methods. 2015;12:7–8.
72. Overmann J, Coolen MJL, Tuschak C. Specific detection of different phylogenetic groups of chemocline bacteria based on PCR and denaturing gradient gel electrophoresis of 16S rRNA gene fragments. Arch Microbiol. 1999;172:83–94.
73. Mori Y, Purdy KJ, Oakley BB, Kondo R. Comprehensive detection of phototrophic sulfur bacteria using PCR primers that target reverse dissimilatory sulfite reductase gene. Microbes Environ. 2010;25:190–6.
74. Finneran KT, Johnsen CV, Lovley DR. *Rhodoferax ferrireducens* sp. nov., a psychrotolerant, facultatively anaerobic bacterium that oxidizes acetate with the reduction of Fe(III). Int J Syst Evol Microbiol. 2003;53:669–73.
75. Falagán C, Johnson DB. *Acidibacter ferrireducens* gen. nov., sp. nov.: an acidophilic ferric iron-reducing gammaproteobacterium. Extremophiles. 2014;18:1067–73.
76. Watanabe T, Kojima H, Fukui M. Complete genomes of freshwater sulfur oxidizers *Sulfuricella denitrificans* skB26 and *Sulfuritalea hydrogenivorans* sk43H: genetic insights into the sulfur oxidation pathway of betaproteobacteria. Syst Appl Microbiol. 2014;37:387–95.
77. Kuever J. The family *Desulfobacteraceae*. In: Rosenberg E, DeLong EF, Lory S, Stackebrandt E, Thompson F, editors. The Prokaryotes: Deltaproteobacteria and Epsilonproteobacteria. Berlin Heidelberg: Springer; 2014. pp. 45–73.
78. van Grinsven S, Damsté JSS, Asbun AA, Engelmann JC, Harrison J, Villanueva L. Methane oxidation in anoxic lake water stimulated by nitrate and sulfate addition. Environ Microbiol. 2019;22:766–82.
79. van Grinsven S, Damsté JSS, Harrison J, Villanueva L. Impact of electron acceptor availability on methane-influenced microorganisms in an enrichment culture obtained from a stratified lake. Front Microbiol. 2020;11:715.
80. Kappler A, Bryce C. Cryptic biogeochemical cycles: unravelling hidden redox reactions. Environ Microbiol. 2017;19:842–6.
81. Walter XA, Picazo A, Miracle MR, Vicente E, Camacho A, Aragno M, et al. Phototrophic Fe(II)-oxidation in the chemocline of a ferruginous meromictic lake. Front Microbiol. 2014;5:713.
82. Allen JWA, Sawyer EB, Ginger ML, Barker PD, Ferguson SJ. Variant *c*-type cytochromes as probes of the substrate specificity of the *E. coli* cytochrome *c* maturation (Ccm) apparatus. Biochem J. 2009;419:177–86.
83. He S, Lau MP, Linz AM, Roden EE, McMahon KD. Extracellular electron transfer may be an overlooked contribution to pelagic respiration in humic-rich freshwater lakes. mSphere. 2019;4:e00436–18.
84. Guzman MS, Rengasamy K, Binkley MM, Jones C, Ranaivoarisoa TO, Singh R, et al. Phototrophic extracellular electron uptake is linked to carbon dioxide fixation in the bacterium *Rhodopseudomonas palustris*. Nat Commun. 2019;10:1355.
85. Croal LR, Jiao Y, Kappler A, Newman DK. Phototrophic Fe(II) oxidation in an atmosphere of H_2: implications for Archean banded iron formations. Geobiology. 2009;7:21–4.
86. Chan C, McAllister SM, Garber A, Hallahan BJ, Rozovsky S. Fe oxidation by a fused cytochrome-porin common to diverse Fe-oxidizing bacteria. bioRxiv. 2018. https://doi.org/10.1101/228056.
87. Daye M, Klepac-Ceraj V, Pajusalu M, Rowland S, Farrell-Sherman A, Beukes N, et al. Light-driven anaerobic microbial oxidation of manganese. Nature. 2019;576:311–4.
88. Petersen TN, Brunak S, von Heijne G, Nielsen H. SignalP 4.0: discriminating signal peptides from transmembrane regions. Nat Methods. 2011;8:785–6.
89. Pettersen EF, Goddard TD, Huang CC, Couch GS, Greenblatt DM, Meng EC, et al. UCSF Chimera—a visualization system for exploratory research and analysis. J Comput Chem. 2004;25:1605–12.